photonics

Article

X-Optogenetics and U-Optogenetics: Feasibility and Possibilities

Rachel Berry [†]**, Matthew Getzin** [†]**, Lars Gjesteby and Ge Wang** *

The Department of Biomedical Engineering, Rensselaer Polytechnic Institute, Troy, NY 12180, USA;
E-Mails: berryr2@rpi.edu (R.B.); matthew.getzin@gmail.com (M.G.); gjestl28@gmail.com (L.G.)

[†] Rachel Berry and Matthew Getzin contributed equally to this work.

* Author to whom correspondence should be addressed; E-Mail: wangg6@rpi.edu;
 Tel.: +1-518-698-2500.

Abstract: Optogenetics is an established technique that uses visible light to modulate membrane voltage in neural cells. Although optogenetics allows researchers to study parts of the brain like never before, it is limited because it is invasive, and visible light cannot travel very deeply into tissue. This paper proposes two new techniques that remedy these challenges. The first is x-optogenetics, which uses visible light-emitting nanophosphors stimulated by focused x-rays. X-rays can penetrate much more deeply than infrared light and allow for nerve cell stimulation in any part of the brain. The second is u-optogenetics, which is an application of sonoluminescence to optogenetics. Such a technique uses ultrasound waves instead of x-rays to induce light emission, so there would be no introduction of radiation. However, the tradeoff is that the penetration depth of ultrasound is less than that of x-ray. The key issues affecting feasibility are laid out for further investigation into both x-optogenetics and u-optogenetics.

Keywords: Optogenetics; x-rays; ultrasound; nanophosphors; penetration depth

1. Introduction

After a transformative approach is invented, there is often a period of improvements and optimizations that expands the reach of the technology. Optogenetics, an incredibly innovative method that allows for deep insight in the field of neuroscience and neuropathology, falls into this category of innovations. Since its introduction into mainstream science less than 20 years ago, a number of teams

have adopted the technique to study the roles of various neurons in disease states such as Parkinson's, epilepsy, and depression [1]. However, these applications are limited in their scopes because of the invasive nature and depth limitation of optogenetics. There is a critical and immediate need to improve optogenetics for deeper and non-invasive applications.

In this paper, we will briefly review the optogenetics techniques focusing on the areas that need improvements, and introduce two possible enhancements that seek to eliminate invasiveness and overcome depth limitations. One of our proposed techniques takes advantage of the recent advances in both nanomaterials and x-ray optics. A synergistic combination, x-optogenetics can deeply target nerves without any surgical intervention. The other method aims to take advantage of methods previously demonstrated *in vivo* that produce ultrasonic-induced luminescence without radiation [2]. Both methods offer transformative improvements to what is already a powerful technology.

Optogenetics

Optogenetics refers to the technology that uses visible light to trigger changes in proteins that modulate membrane potentials in neuronal cells through excitatory or inhibitory membrane currents [3]. This ability to modulate neuronal cells has proven instrumental in preclinical studies and holds enormous potential for the treatment of diseases such as Parkinson's, epilepsy, and depression [1]. However, the current techniques used for optogenetic control remain too invasive for clinical applications. These techniques are briefly described below to offer the motivation behind our innovative ideas for advancing their efficiency and scope.

Created by Karl Deisseroth, the original form of optogenetics uses channelrhodopsin2 (ChR2) to induce excitatory potentials in transfected neurons of small animals. ChR2 is a transmembrane ion channel found in green algae that becomes permeable to cations in the presence of blue light. Deisseroth rationalized that ChR2 could be used in neurons because ion channels are a main contributor in electrical signal transduction in the brain. Since then, the technology has allowed researchers to target specific areas of the brain and study how modulated neuron firing affects downstream behaviors and cellular processes [4,5]. Additionally, other light sensitive transmembrane proteins which also regulate the transmembrane voltage by maintaining ion concentrations on either side of the membrane have been identified and used in the field of optogenetics. Halorhodpsin (NphR) and archeorhodopsin (Arch) are two such proteins and are called ion pumps. Both channels and pumps can be further generalized into the protein group called rhodopsins.

Optogenetics is performed in multiple steps: first, specified neuronal cells are transfected with DNA encoding for the appropriate rhodopsin for the application. Upon expression of these proteins, scientists surgically implant a light fiber into the organism's brain so light at the stimulating wavelengths can directly irradiate neurons and modulate their membrane current. Such current modulation comes in two forms that depend on the ions to which the channel becomes permeable in its open state. The cation-specific channels lead to membrane depolarization (excitatory) and the proton/anion-specific pumps cause the membrane to hyperpolarize (inhibitory) [3].

In this way, the membrane current is directly controlled by a light source which is currently in the form of either a laser or a LED. Both sources have limitations. Lasers are very costly. On the other hand, the light from a LED is spread out and not a straight beam, so it cannot be accurately targeted as

laser can [6–9]. It should be noted that current practice of optogenetics is performed on a macroscopic scale. For example, ChR2-expressing cells have been activated by a 470–490 nm light in power range 1–20 mW/mm^2 and pulse duration 5–100 ms. This type of stimulation results in ChR2-channel driven membrane current that peaks around −9 pA/pF [6–8,10]. In these experiments, the studied tissue is flooded with light and any cell within a few millimeters of the source that is expressing rhodopsins will have modulated membrane currents that may lead to distinct network and/or behavioral changes. The proposed x-optogenetic and u-optogenetic techniques shift the scale from the macroscopic to a microscopic or even nanoscopic level of control. This will become more apparent in the following sections.

Because of the invasive nature or limited penetration of LEDs and laser sources, researchers are trying to find light sources that do not require surgical implantation and that deliver light more deeply. For example, Dr. Gang Han uses near infrared radiation to excite upconversion nanoparticles (UCNPs) [11]. After excitation, these nanoparticles will emit photons of visible light whose wavelengths can be customized based on the particle chemistry. These emissions are then used to modulate the membrane current just as the light sources described above. This method offers a unique and less invasive approach to optogenetics as deeper levels of the brain can be mapped due to the deeper penetrating abilities of infrared light [11]. Table 1 lists a number of these light-emitting nanoparticles (nanophosphors) which have been reported in the literature and may have utility in this regard. Despite this incremental improvement to the optogenetic approach, infrared (IR) light has its limitations as well. First, IR penetration through the skull has been shown to be between 4% and 10% of the initial intensity [12]. Furthermore, IR light at 868 nm only penetrates brain tissue around 2.5 mm [13], which can only gain access to a fraction of human cortical neurons, as the human cortex thickness is typically in the range of 2–5.5 mm [14]. We believe that these challenges can be addressed through the use of x-rays, rather than infrared light, to stimulate nanophosphors. X-rays are capable of very deep penetration and can also be precisely focused as is discussed below. Due to the radiation dose introduced by x-rays, we also explore the possibility of ultrasonic stimulation of air bubbles that emit light via sonoluminescence. This technique would not introduce radiation to the subject, but the penetration depth would not be as high as that of x-ray stimulation methods.

2. Methodology

2.1. Key Elements for X-Optogenetics

2.1.1. X-Ray Excitable Nanophosphors

To perform x-optogenetics, the x-rays must be converted to visible light; therefore, x-ray excitable nanophosphors must be used. Specific nanophosphors can absorb x-ray light which promotes a number of resident electrons to higher energy orbitals. These electrons then quickly revert back to their ground-state, emitting light with energy equal to the band gap between the two orbitals in the process [15]. If these nanophosphors are targeted to the rhodopsins inserted into the brain, then the emitted visible light can be close enough to change the properties of the rhodopsins to perform optogenetics. Although the use of nanophosphors are an additional step needed in x-optogenetics which is not seen in traditional optogenetics, it is a beneficial tool that will allow optogenetics to be performed deeper into tissue.

The nanophosphors ought to be biocompatible and emit light at wavelengths that properly activate the light sensitive ion channels/pumps. This idea was recently used as the basis of a patent application, though it simply describes using x-ray excitable nanophosphors for general "control of light-sensitive bioactive molecules" without any quantitative analysis of feasibility or radiation dose implications [16]. A literature survey of nanophosphors verified that a large number of nanophosphors can be readily produced with tunable emission, absorbance, and solubility properties. Table 1 shows a large number of nanophosphors with emission maxima in the visible domain. With regards to their excitation spectra, however, two distinct types of nanoparticles can be seen: up-conversion nanoparticles (UCNPs) and UV/x-ray excitable nanoparticles. As stated above, UCNPs emit visible photons during exposure to long wavelength infrared radiation, while the UV/x-ray excitable particles emit visible photons during exposure to short wavelength UV/x-ray radiation. It should be noted that particles in the same conversion class are often doped with similar ions. For example, UCNPs often contain Yb^{3+}, Ln^{3+}, or Er. On the other hand, particles sensitive to the shorter wavelength radiation often contain Cr^{3+}, Eu^{3+}, or Tb^{3+}.

Of the reported nanophosphors, most have the excitation wavelength in the range from 147–980 nm. There are five nanophosphors in the survey with an excitation wavelength of 980 nm all of which are upconverting nanoparticles (UCNPs). X-rays have a wavelength range from 0.01–10 nm [17] and therefore cannot efficiently excite these nanophosphors. However, the particles with the base chemistry of Gd_2O_2S and $LiGa_5O_8$ have been shown to absorb light in both the UV and x-ray ranges. Additionally, these particles have been doped with Cr^{3+}, Eu^{3+}, or Tb^{3+}. Other particles in the survey also utilize these dopants and may also prove to be useful for x-ray excitation. Further research should generate optimal nanophosphors for x-optogenetics.

The results from the literature suggests that there are a number of techniques available to improve the nanophosphors that can be used for x-optogenetics, especially in the areas of solubility, conversion efficiency, emission, size, and targeting. For example, Table 1 includes nanophosphors that emit light across the visible light spectrum and into the NIR range with the shortest wavelength emitted at 450 nm and the longest at 800 nm. The emission wavelength is a result of the chemical formula of the nanophosphor and the compound with which it is doped. For example, $NaYF_4$ doped with Eu^{3+} has an emission wavelength of 592 nm while $NaYF_4$ doped with Tb^{3+} has an emission wavelength of 545 nm. The ability to alter a nanophosphor's emission wavelength by changing the chemical formula or the compound with which it is doped should be beneficial in optimizing nanophosphors for x-optogenetics. Hybrid doping schemes may also allow for more tailored emission spectra.

The conversion efficiency is the ability for the nanophosphors to convert x-ray energy to visible light energy. This value was not expressed for many of the nanophosphors, though it remains an important consideration for x-optogenetic applications. When choosing a nanophosphor for x-optogenetics, the conversion efficiency should be as high as possible to reduce the amount of time and x-ray dose to which the subject is exposed. It is underlined that we consider x-ray stimulation feasible and safe, given the extensive research on x-ray luminescence imaging in preclinical applications [18].

Table 1. Survey of nanophosphors in the literature. Italicized entries represent nanophosphors which may be useful for x-optogenetics as Eu^{3+} and Tb^{3+} are common dopants for x-ray excitable nanophosphors. Not all of these particles reported x-ray induced fluorescence (PEG – polyethylene glycol, PAA – poly(acrylic acid), PGA – polyglycolic acid, PEI – polyethylenimine, DSPE-PEG-COOH–1,2-distearoyl-sn-glycero-3-phosphoethanolamine-N-[carboxy(polyethylene glycol)]).

Formula	Source	Emission Maximum (nm)	Excitation Wavelength (nm)	Conversion Efficiency (%)	Size (nm)	Dispersible	Toxicity
$Gd_2O_2S:Eu^{3+}$ (Tb^{3+})	[19–22]	*620 (545)*	*<310*	*15*	*50–300*	*Yes, PGA-PEG*	*Low*
$Y_2O_3:Eu^{3+}$	[23–25]	*610*	*<310*	*80*	*10–50*	*Yes*	*--*
$LiGa_5O_8:Cr^{3+}$	[26,27]	*716*	*<310*	*--*	*50–150*	*Yes, PEI*	*Low*
$Gd_2O_2S:Yb(8),Er(1)$	[28]	500–700	980	25	4 μm	Yes	Low
$NaMF_4:Yb^{3+}/Ln^{3+}$	[29]	510–560	980	--	60	Yes, DSPE-PEG-COOH	Low
$La(OH)_3:Eu^{3+}$	[30]	*597, 615*	*280*	*--*	*3.5*	*Yes, PEG*	*Low*
$NaYF_4:Yb/Er$	[31]	520, 540, 654	980	--	33 ± 1	Yes, citrate	--
$NaYF_4:40\%Eu^{3+}$	[32]	*592*	*394*	*--*	*28*	*Yes, PAA*	*Low*
$NaYF_4:40\%Tb^{3+}$	[32]	*545*	*368*	*--*	*28*	*Yes, PAA*	*Low*
cit-$NaLuF_4:Yb,Tm$	[33]	800	980	--	25	Yes, citric acid	Low
Ba_2SiO_4	[34]	505	350	38.6	40–50	--	--
$Na_2Sr_2Al_2PO_4F_9:Eu^{3+}$	[35]	*593, 619*	*393*	*--*	*35.26*	*--*	*Non-toxic materials*
$BaMgAl_{10}O_{17}:Eu^{2+}$	[36]	*450*	*147*	*--*	*62, 85, 115, 160, 450*	*--*	*--*
Sr_2CeO_4	[37]	467–485	240–360	--	45	--	--
$LiCaPO_4:Eu^{2+}_{0.03}$	[38]	*476*	*375*	*Quantum Efficiency: 53.7, 67.6*		*Yes, PEG-P*	*--*
$PEG-Er-Y_2O_3$	[39]	660	980	--	30–60	Yes, PEG	Low
$GdVO_4:Eu^{3+}$	[40]	*620*	*330*	*--*	*6*	*Yes*	*Low*

When considering x-optogenetics for neuronal intervention, the size distribution and coating of the nanophosphors are important for penetration of the phosphors across the blood brain barrier (BBB) to gain access to the cells in the brain. Sizes of particles targeted outside of the central nervous system do not need to be as small, but should still be optimized for maximum bioavailability. Studies using polysorbate-coated nanoparticles showed maximum passage through the BBB for nanoparticles under 100 nm in diameter [41]. Given the sizes of the nanophosphors in the survey between 10 nm and 1 μm and recent advances in nanotechnology, it should be feasible to obtain nanophosphors with an appropriate size distribution for a range of x-optogenetic applications [42].

In addition to size, the ability for the particles to be soluble or colloidal in water is a critical property of the nanophosphors as this should add to their biocompatibility. A number of surface coatings including polyethylene glycol (PEG) and other forms of hydrophilic polymers were used to

solubilize or suspend the surveyed particles in aqueous solutions. These types of coatings could be used for the nanophosphors to facilitate x-optogenetics. These coatings can also have a profound effect on the ability of the particles to cross the blood brain barrier [41].

2.1.2. Nanoparticle Targeting

One important aspect of x-optogenetics is the placement of the light sources that will be used to generate membrane current in the target neurons. The proximity of these nanophosphors in relation to the rhodopsins must be within very short distances as power density is reduced by >90% after 1 mm for all wavelengths of visible light [43].

One way of combatting this light loss through tissue would be to directly target the light-sensitive ion channels/pumps through functionalization of the nanoparticles. Several groups have demonstrated the ability to conjugate small peptide sequences or antibodies that can be used to enhance cellular uptake or adhesion to the cellular membrane [44–46]. Using similar methods, the nanophosphors could be functionalized to specifically bind to the rhodopsins expressed by the target neurons. Specifically, monoclonal antibodies showing specificity toward ChR2 antigens can be produced by a number of proprietary companies. These antibodies can then be conjugated to the nanophosphors by reacting their free amine group with the carboxylic acid coating of the nanophosphors. In this way, the proximity issue between the light-sensitive ion channels and the light sources can be minimized, and the light loss due to tissue absorption mitigated.

2.1.3. X-Ray Focusing

Targeting the genetically-modified neurons through functionalization of the nanophosphors will provide the first level of control for neuron activation. A second level of control comes from the ability to focus x-rays through the use of a polycapillary lens, a zone plate, or another similar means such as a grating. In addition to enhanced control over the neuronal activation, focused x-rays will result in less bulk x-ray dose to the patient which is always of high concern when dealing with ionizing radiation.

A polycapillary lens focuses x-rays in the form of an intense microspot using an array of glass micro-capillaries. The size of the focal spot can be as low as 5 μm [47]. However, for single neuron targeting focal spots of a few 100 μm may be more applicable. Conventional polycapillary lenses have a working energy range of 0.5–30 keV. These can be described as soft x-rays and more easily absorbed by the brain tissues. Also, polycapillary optics has recently been made for focusing of higher energy x-rays up to 60 keV, although transmission through these lenses is <5% at energies higher than 5 keV [48].

Excitation of x-ray excitable nanophosphors using the same mechanisms has been previously proposed and simulated by our group [49]. As described for x-ray fluorescence computed tomography (XFCT) applications, the x-ray intensity distribution in biological soft tissues can be approximated with inverse distance weighting. In this approximation, $I(\boldsymbol{r}) = I_0 W(\boldsymbol{r}, \boldsymbol{r}_0)/\|\boldsymbol{r} - \boldsymbol{r}_0\|^2$, where $\mathbf{r}_0$ is the vertex of the double cones, I_0 is the intensity of the x-ray source, and $W(\mathbf{r},\mathbf{r}_0)$ is the aperture function of the double cones at the vertex $\mathbf{r}_0$. For accurate membrane current modulation of the target neurons, the initial intensity of the x-ray source can be adjusted so that the nanophosphors near $\mathbf{r}_0$ will receive enough x-ray energy to emit a sufficient number of light photons to activate the rhodopsins. This

real-time adjustment also depends on the location of the target neurons as well as the size and fluorescence conversion efficiency of the nanoparticles.

Focusing x-rays can be more precise through the use of a Fresnel zone plate (FZP). FZPs are micro-fabricated from a soft metal such as gold or nickel, and modulate either amplitude or phase-shift of incoming x-rays. These modulations result in a wave diffraction and constructive interference at a focal point [50]. One consideration is that zone plates are typically used for synchrotron produced x-rays. Similar to the polycapillary lens, zone plates are most effective for x-rays with lower energy levels (5–8 keV) [50]. All things considered, the polycapillary lens may be initially the best option for x-optogenetics.

Table 2. X-optogenetic overview for multiple light-sensitive ion channels/pumps. Included in this table are approximate sizes of the channels/pumps which help validate close proximity of nanophosphors and channels/pumps after targeting. Furthermore, nanoparticles for targeting the ion channels/pumps are specified.

Ion Channel/Pump	Channelrhodopsin 2 (ChR2)	Halorhodopsin (NphR)	Archeorhodopsin (Arch)
Channel/Pump Mass	30 kDa [51]	30 kDa [52]	28 kDa [53]
Minimum Channel/Pump Radius (assuming spherical)	2.58–2.72 nm [54]	2.05 nm [54]	2.00 nm [54]
Intensity	2–20 mW/mm^2 [55]	5.4 $\pm$0.2 mW/mm^2 [56]	<10 mW/mm^2 [56]
Wavelength	488 nm [55]	532 nm [57]	532 nm [57]
Pulse Train	5 ms, 40 Hz [55]	15 s illumination [57]	15 s illumination [57]
Depolarizing/Hyperpolarizing	Depolarizing	Hyperpolarizing	Hyperpolarizing
Possible Nanophosphors	*BaMgAl$_{10}$O$_{17}$:Eu^{2+}* *LiCaPO$_4$:Eu$^{2+}_{0.03}$*	*Gd$_2$O$_2$S:Tb^{3+}* *(combination doping?)*	*Gd$_2$O$_2$S:Tb^{3+}* *(combination doping?)*
Hardware Specifications/Involved Components	SOURCE: Carbon Nanotube (peak ~8 keV, pulsing capability) FOCUSING ELEMENT: polycapillary lens OR Fresnel zone plate		

2.1.4. X-ray Carbon Nano-Tube (CNT) Sources

Another key aspect of optogenetics that must be addressed by x-optogenetics is the delivery of light in pulses 5–100 ms in duration. With the light emitted from the nanophosphors as they are excited by x-rays, the pulsation must come from the x-ray source itself. Conventional tubes emit x-rays under 10–500 mA current and require several minutes for warming-up before emission. Achieving a sufficient pulsing emission rate will not be possible with such a source. Fortunately, recent progress has been made on the development of carbon-nanotube field-emission cathodes that can produce soft x-rays and are capable of pulsing at high rates for x-optogenetics research and application [58].

2.1.5. X-Ray Dose

With the involved ionizing radiation for x-optogenetics, it is important to quantify the delivered radiation dose during a procedure. While everyone is subject to a baseline effective dose of about 3 mSv a year, increased levels of radiation exposure occur as a result of x-ray radiography, CT, and PET/SPECT imaging exposure. The effective dose from such a scan can range anywhere from 0.001 mSv–25 mSv. These values depend on the region of exposure, type of radiation, and type of scan. For x-ray related scans, a highest effective dose administered is around 10 mSv [59]. We will use this number as the highest effective dose permissible for x-optogenetics protocols in the following feasibility analysis.

2.2. X-Optogenetics Safety Analysis

Table 2 summarizes the requirements for the various rhodopsins in past studies. As stated previously, these techniques take a macroscopic view of optogenetics. When considering the requirements for x-optogenetics, a micro/nanoscopic scale must be used. The nanophosphors must be excitable with x-rays, be biocompatible, and have a high conversion efficiency. Depending on the nanophosphors used, the x-ray dose may be adjusted. In any case, the nanophosphors should emit visible light that can be used for optogenetics. A CNT, polycapillary lens, Fresnel zone plate or a similar component should be used to deliver x-rays.

Assuming a maximum effective radiation dose of 10 mSv, a theoretical calculation of power emitted from the nanophosphors chosen from Table 2 can be performed. For x-ray radiation, a Sievert (Sv) is defined as 1 Joule (J) of energy per kilogram (kg) of tissue. By definition, 1 J is equal to 6.24 E 12 MeV [60]. Furthermore, Chen *et al*. reported that the conversion efficiency of the Gd_2O_2S particles to be about 60,000 visible photons per MeV of absorbed x-ray energy [20]. Using these relationships, the following conversion can be done.

$$0.010\ Sv\left(\frac{1\frac{J}{kg\ tissue}}{1\ Sv}\right)\left(\frac{6.24E12\ MeV}{1\ J}\right)\left(\frac{60000\ photons}{1\ MeV}\right) = 3.744E6\frac{photons}{\mu g\ tissue}$$

This conversion is the approximation of photons absorbed per microgram of brain tissue. Then, let us approximate the number of photons per nanophosphor. According to the manufacturer, there are about 3.25×10^{13} nanophosphors per gram or 3.25×10^7 per microgram. Using these assumptions, another conversion can be performed.

$$3.744E6\frac{photons}{\mu g\ tissue}\left(\frac{\mu g\ tissue}{3.25E7\ nanophosphors}\right) = \frac{0.1152\ photons}{nanophosphor}$$

Less than one photon per nanophosphor is not enough to activate a single rhodopsin. However, two of the initial assumptions can be altered to greatly enhance the number of photons per nanophosphor. The first is the phosphor diameter. The nanophosphor mass used in the equation was for 50 nm diameter nanophosphors. Simply by increasing the nanophosphor diameter by a factor of 3 (150 nm), the nanophosphor mass will be increased by 27 times (3^3), assuming the material density is constant. Increasing the mass results in a proportional decrease of the number of nanophosphors per microgram, yet the conversion efficiency and input energy remain constant. Therefore, output emission is boosted

to 3 photons per nanophosphor (H. Chen, personal communication, November 20, 2014). Further improvement can be achieved by increasing the conversion efficiency of the nanoparticles. The current conversion factor (60,000 photons/MeV) is only 15% as there is enough energy to generate ~400,000 visible photons (496 nm) in one MeV. Therefore, every 5% increase in efficiency is equal to an increase of 20,000 photons. With both of these adjustments, phosphors with a diameter of 150 nm and a quantum efficiency of 50% will emit more than **10 photons per nanophosphor under the acceptable x-ray dose**.

The second part of the feasibility analysis is the number of light photons needed to open the light-activated ion channel/pumps. To approximate this number, an understanding of the gating mechanism in the proteins is necessary. The light-sensitive moiety of all rhodopsins is a covalently bound derivative of Vitamin A, retinal, that isomerizes under light excitation. According to Hegemann and Möglich, the sensitivity of rhodopsins are defined in part by the quantum efficiency of retinal. This is described as the likelihood of the chromophore to isomerize after absorption of a single photon of light. This efficiency falls between 30% and 70% in rhodopsins [61]. With this in mind, a single rhodopsin will need between **1.5 and 3 photons of absorbed light to isomerize the retinal molecule and trigger activation of the protein**. As calculated above, by increasing the radius of the particles alone, sufficient numbers of photons can be generated to activate the rhodopsins.

2.3. U-Optogenetics via Sonoluminescence

Sonoluminescence was first discovered in 1934 when air bubbles in a photo-developing solution were seen to emit short bursts of light when subjected to ultrasonic waves [62]. This sonoluminescence effect is due to a cavitation process in which bubbles fill with gas and vapor. Under ultrasonic waves of a specific pressure, collisions between free electrons and ions in the air bubbles cause them to collapse, and these collisions result in thermal bremsstrahlung radiation from electron deflections, which is released as a short burst of light [63]. Studies have shown that the sonoluminescence effect can be enhanced by the introduction of a chemiluminescent agent, such as fluoresceinyl Cypridina luminescent analog (FCLA), which reacts with oxygen free radicals in air bubbles to emit luminescence [2]. FCLA achieves its effect by interacting with reactive oxygen species that result from ultrasonic waves passing through tissue, and this interaction causes a release of chemical energy that alters the structure of FCLA [64]. Structural changes induce FCLA molecules into a brief excited state, and the subsequent relaxation results in an emission of photons [64]. Under ultrasonic waves with a pressure of 200 kPa, FCLA molecules dissolved in water were reported to emit strong chemiluminescence at a peak wavelength of 532 nm with an intensity of 12,580 photons cm^{-2} s^{-1} in a mouse model [2]. This characteristic presents an ideal emission wavelength for use in optogenetics, namely u-optogenetics. FCLA would need to be targeted close to rhodopsins using a method similar to what was previously mentioned for x-ray excitable nanophosphors. When subjected to ultrasonic waves, the collapsing air bubbles interacting with FCLA would emit bursts of light to trigger the activation of select rhodopsins.

Figure 1B illustrates the use of sonoluminescence to stimulate the ion channels. Under these conditions, sonoluminescence provides an alternative excitation pathway in optogenetics. The advantage of ultrasound over x-ray methods is that no radiation dose would be introduced to the patient. However, there is greater attenuation of ultrasonic waves in tissue and bone as compared to

x-rays, so penetration depth would be limited. By using low frequency ultrasound waves, penetration depth can be maximized. For ultrasound waves with a frequency of 1 MHz, the penetration depth in bone is approximately 0.3 cm; at a wave frequency of 100 kHz, the penetration depth would increase to approximately 3 cm [65]. Further, a new study has been reported that may enable even greater penetration depths for ultrasound through the skull by use of acoustic complementary metamaterials that can cancel out aberrating layers in bone, which could be relevant to scaffold-based experiments [66].

The feasibility of u-optogenetics depends mainly on the ability of FCLA, or another chemiluminescent agent, to target ion channels and pumps directly, though we hypothesize that similar methods to those outlined for nanophosphor targeting can be used. Ultrasonic stimulation provides a non-invasive way to stimulate light emission with greater depth than traditional optogenetics. U-optogenetics also has an advantage over x-optogenetics by not delivering ionizing radiation, but it does not equal the penetration distance and focusing power of x-ray techniques.

3. Discussions and Conclusions

Putting the pieces together, x-optogenetics seems to be a promising approach beyond the currently accepted optogenetic techniques. Figure 1A illustrates the combination of the key elements for x-optogenetics as described in the Methodology section. By replacing the light sources in the form of lasers or LED with x-ray excitable nanophosphors, the issues of invasiveness and depth-limitedness of optogenetic stimulation can be addressed. Through functionalization of the nanoparticles, a desirable targeting capability can be achieved that will allow for accumulation of the nanophosphors near the rhodopsins. When choosing the nanophosphors, those with high energy conversion efficiency will be preferred as they will work with lower x-ray dose, given the maximum power emission for cell stimulation. Furthermore, the size distribution of nanoparticles will also affect the dose needed to achieve sufficient visible light emission. Polycapillary lenses or zone plates can be used to focus x-rays onto altered cells. The x-ray flux will directly affect the density of the emitted light. Through the use of a carbon nano-tube x-ray source rather than a conventional source, a high level of temporal control can be implemented over x-ray excitation, inducing luminescence pulses from the nanophosphors at suitable frequencies and duty cycles.

X-optogenetics is a feasible idea since it uses a safe x-ray dose to excite nanophosphors allowing photon emission that will be able to reach and activate targeted rhodopsins. As previously stated, there will be enough photons to activate the rhodopsins if the radius and/or conversion efficiency of the nanophosphor is increased. It should be noted that increasing the radius of the nanophosphor will lead to additional considerations. For example, the nanophosphor must be small enough to pass through the blood brain barrier (BBB); therefore, increasing the nanophosphor radius could decrease the nanophosphor penetration through the BBB. Optimization of the size distribution, particle emission, and BBB penetration will be a key consideration moving forward with x-optogenetics. If it is determined that the nanophosphor's radius is increased by more than what would pass through the BBB, x-optogenetics could also be applied to other regions of the body [67].
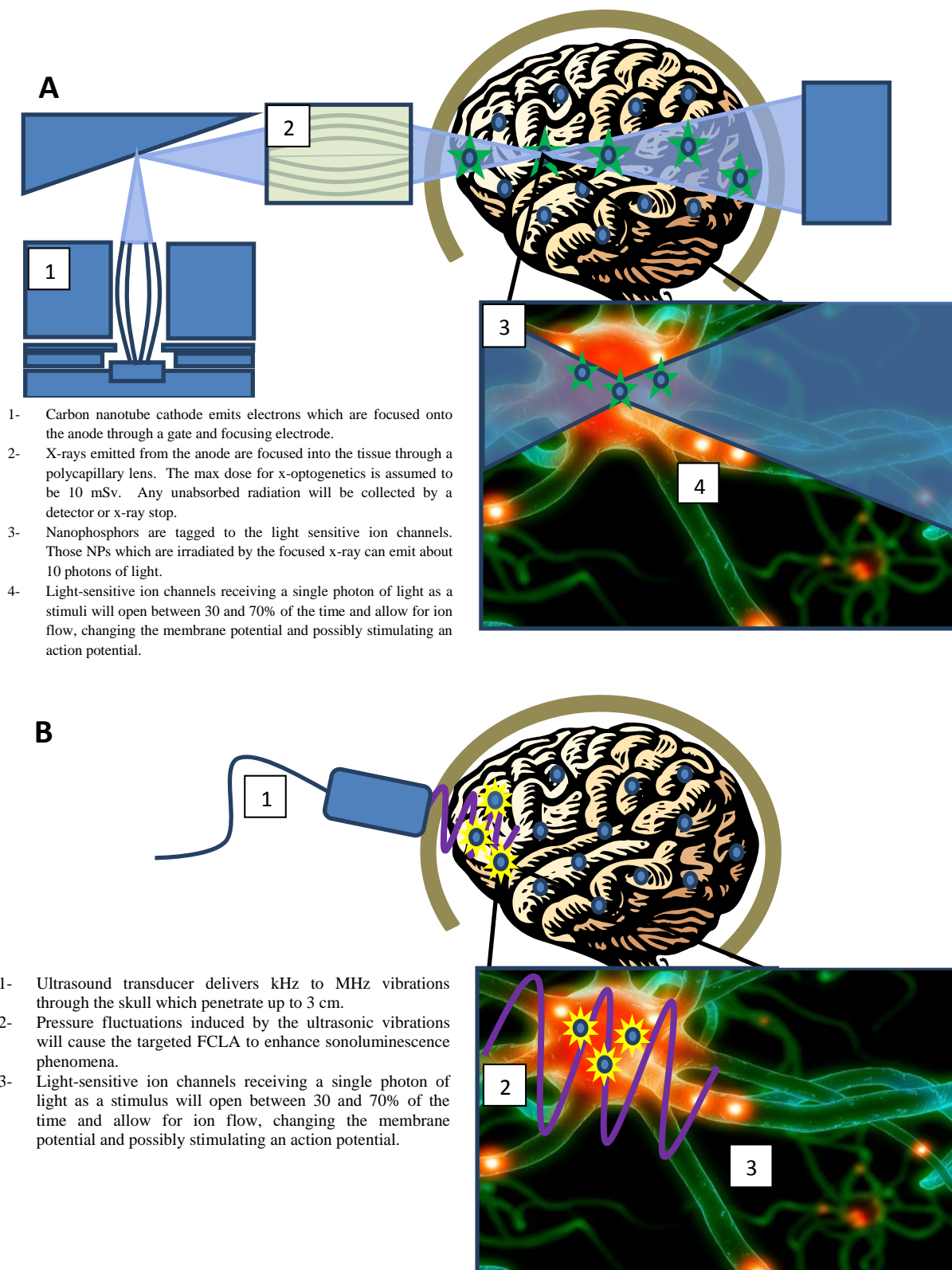
A

1- Carbon nanotube cathode emits electrons which are focused onto the anode through a gate and focusing electrode.
2- X-rays emitted from the anode are focused into the tissue through a polycapillary lens. The max dose for x-optogenetics is assumed to be 10 mSv. Any unabsorbed radiation will be collected by a detector or x-ray stop.
3- Nanophosphors are tagged to the light sensitive ion channels. Those NPs which are irradiated by the focused x-ray can emit about 10 photons of light.
4- Light-sensitive ion channels receiving a single photon of light as a stimuli will open between 30 and 70% of the time and allow for ion flow, changing the membrane potential and possibly stimulating an action potential.

B

1- Ultrasound transducer delivers kHz to MHz vibrations through the skull which penetrate up to 3 cm.
2- Pressure fluctuations induced by the ultrasonic vibrations will cause the targeted FCLA to enhance sonoluminescence phenomena.
3- Light-sensitive ion channels receiving a single photon of light as a stimulus will open between 30 and 70% of the time and allow for ion flow, changing the membrane potential and possibly stimulating an action potential.

Figure 1. (**A**) Schematic of X-optogenetics showing the use of a CNT source as well as a polycapillary lens for x-ray focusing into a double-cone geometry. CNT source schematic was adapted from Zhang *et al*. [69]. (**B**) Schematic of U-optogenetics that heuristically demonstrates use of ultrasound to induce sonoluminescence and modulate membrane potential. Brain and neuronal cell images were sourced from Microsoft clipart.

Additionally, the importance of targeting x-ray excitable nanophosphors to the rhodopsins should be noted. The closer the nanophosphors are to the rhodopsins, the more photons there will be that are able to activate them. Therefore, the nanophosphors should be targeted to the rhodopsins as specifically as possible. It is likely that only a small number of the proteins will be directly targeted by the nanophosphors relative to the number expressed in a given cell. This may have a substantial impact on the ability for x-optogenetics to have macroscopic and behavioral effects.

In most optogenetic studies, the light stimuli are delivered in sub-second pulse trains over relatively longer periods. We have discussed the importance of using the CNT for having millisecond control over the x-ray delivery; however, in the feasibility analysis the whole dose, is assumed to be delivered in a single pulse. Clearly, administering an x-ray pulse train of 10 mSv each greatly increases the total effective dose, putting the subject at risk for radiation damage. However, a recent study has looked into the inhibitory effects of ChR2-based mutants after a single light pulse [68]. These variants can have effects that outlast the light stimulus. Therefore, x-optogenetics remains a feasible option for these rhodopsin variants since a single x-ray dose resulting in a single light stimulus will cause lasting membrane voltage modulation in the target neurons.

U-optogenetics via sonoluminescence provides a second alternative method to stimulating ion channels without the need for implanted light sources. This technique differs from x-optogenetics in that it relies on ultrasonic waves as the medium for inducing light emission, instead of x-rays, and therefore does not introduce a radiation dose. The penetration depth and focusing power of u-optogenetic techniques would not be as high as with x-optogenetic methods, but 3 cm penetration depth through the skull using 100 kHz ultrasonic waves would still offer a substantial advantage over traditional optogenetics. Sonoluminescence would be enhanced by a chemiluminescent agent such as FCLA, which would emit bursts of light from air bubbles collapsing under ultrasonic pulses. Targeting of FCLA to ion channels provides a means for direct stimulation, but this mechanism remains an area of further investigation. Furthermore, u-optogenetics will not have the pulse-train limitation as radiation dose is not an issue for this technique.

Without the use of a light probe, x-optogenetics and u-optogenetics turn optogenetics into a less invasive and more applicable research tool. The decreased invasiveness puts optogenetics one step closer to being applied to features deeper into tissue and subjects other than rodents. Additionally, it makes optogenetics a less time-consuming and more ethical process since researchers no longer need to surgically drill into the skull of their subjects. Moreover, the ability for x-optogenetics and u-optogenetics would allow researchers to study parts of the brain that current practice of optogenetics does not allow. This would create a grand opportunity to learn and explore parts of the brain that have yet to be explored as well as other regions of the body.

Author Contributions

Dr. Ge Wang is the corresponding author and produced many of the ideas presented in this paper. Matthew Getzin created the images, wrote a large portion of the paper, and contributed to the conversion calculations for X-optogenetics. Rachel Berry did background research on Dr. Wang's ideas, wrote a large portion of the paper, and contributed to the conversion calculation. Lars Gjesteby wrote and researched about ultrasound, sonoluminescence, and U-optogenetics.

Conflicts of Interest

References

1. Fenno, L.; Yizhar, O.; Deisseroth, K. The development and application of optogenetics. *Annu. Rev. Neurosci.* **2011**, *34*, 389–412.

2. He, Y.; Xing, D.; Tan, S.; Tang, Y.; Ueda, K. *In vivo* sonoluminescence imaging with the assistance of FCLA. *Phys. Med. Biol.* **2002**, *47*, 1535.

3. Optogenetics: Controlling the brain with light. Available online: http://video.mit.edu/watch/optogenetics-controlling-the-brain-with-light-7659/ (accessed on 27 September 2014).

4. Adams, A. Optogenetics earns Deisseroth Keio Prize in Medicine. Available online: https://med.stanford.edu/news/all-news/2014/09/optogenetics-earns-deisseroth-keio-prize-in-medicine.html (accessed on 26 September 2014).

5. Knopfel, T.; Boyden, E.S. *Optogenetics: Tools for Controlling and Monitoring Neuronal Activity*; Elsevier: Oxford, UK, 2012.

6. Grossman, N.; Poher, V.; Grubb, M.; Kennedy, G.; Nikolic, K.; McGovern, B.; Berlinguer, R. Palmini, R.; Gong, Z.; Drakakis, E.; Neil, M.; *et al*. Multi-site optical excitation using ChR2 and micro-LED array. *J. Neural Eng* **2010**, doi:10.1088/1741-2560/7/1/016004.

7. Farah, N.; Reutsky, I.; Shoham, S. Patterned optical activation of retinal ganglion cells. *Conf Proc IEEE Eng Med Biol Soc* **2007**, *2007*, 6368-6370.

8. Lutz, C.; Otis, T.; DeSars, V.; Charpak, S.; DiGregorio, D.; Emiliani, V. Holographic photolysis of caged neurotransmitters. *Nat Methods* **2008**, doi:10.1038/nmeth.1241.

9. Clements, I.P.; Gnadea, A.G.; Rusha, A.D.; Pattena, C.D.; Twomeya, M.C.; Kravitzb, A.V. Miniaturized LED sources for in vivo optogenetic experimentation. *Proc. SPIE* **2013**, *8586*, 85860X–1.

10. Entcheva, E.; Williams, J.C. Channelrhodopsin2 Current During the Action Potential:[ldquo] Optical AP Clamp [rdquo] and Approximation. *Sci. Rep.* **2014**, doi:10.1038/srep05838.

11. Fessenden, J. EUREKA grant to fund development of new "optogenetic" technique for mapping neural networks at UMMS. Available online: http://www.eurekalert.org/pub_releases/2013-10/uomm-egt102413.php (accessed on 26 September 2014).

12. Jagdeo, J.R.; Adams, L.E.; Brody, N.I.; Siegel, D.M. Transcranial red and near infrared light transmission in a cadaveric model. *PLoS One* **2012**, *7*, e47460.

13. Stolik, S.; Delgado, J.A.; Perez, A.; Anasagasti, L. Measurement of the penetration depths of red and near infrared light in human "ex vivo" tissues. *J. Photochem. Photobiol. B Biol.* **2000**, *57*, 90–93.

14. Sowell, E.R.; Thompson, P.M.; Leonard, C.M.; Welcome, S.E.; Kan, E.; Toga, A.W. Longitudinal mapping of cortical thickness and brain growth in normal children. *J. Neurosci.* **2004**, *24*, 8223–8231.

15. Sun, C.; Pratx, G.; Carpenter, C.M.; Liu, H.; Cheng, Z.; Gambhir, S.S.; Xing, L. Synthesis and Radioluminescence of PEGylated Eu^{3+}- doped Nanophosphors as Bioimaging Probes. *Adv. Mater.* **2011**, *23*, H195–H199.

16. Shuba, Y.M. Use of scintillator-based nanoparticles for *in vivo* control of light-sensitive bioactive molecules 2014, Patent US20140219922, 2014.

17. Stark, G. X-ray. Available online: http://www.britannica.com/EBchecked/topic/650351/X-ray (accessed on 27 October 2014).

18. Ahmad, M.; Pratx, G.; Bazalova, M.; Xing, L. X-ray luminescence and x-ray fluorescence computed tomography: new molecular imaging modalities. *IEEE Access* **2014**, doi:10.1109/ACCESS.2014.2353041.

19. Innovation in Dispersible Nanomaterials. Available online: http://www.oceannanotech.com/product.php?cid=92&pid=286 (accessed on 27 October 2014).

20. Chen, H.; Moore, T.; Qi, B.; Colvin, D.C.; Jelen, E.K.; Hitchcock, D.A.; He, J.; Mefford, O.T.; Gore, J.C.; Alexis, F. Monitoring pH-triggered drug release from radioluminescent nanocapsules with X-ray excited optical luminescence. *ACS Nano* **2013**, *7*, 1178–1187.

21. Moore, T.L.; Wang, F.; Chen, H.; Grimes, S.W.; Anker, J.N.; Alexis, F. Polymer-Coated Radioluminescent Nanoparticles for Quantitative Imaging of Drug Delivery. *Adv. Funct. Mater.* **2014**, *24*, 5815–5823.

22. Gorokhova, E.I.; Demidenko, V.A.; Mikhrin, S.B.; Rodnyi, P.A.; Van Eijk, C.W.E. Luminescence and scintillation properties of Gd$_2$O$_2$S: Tb Ce ceramics. *IEEE Trans. Nucl. Sci.* **2005**, *52*, 3129–3132.

23. Jadhav, A.P.; Pawar, A.U.; Pal, U.; Kang, Y.S. Red emitting Y$_2$O$_3$:Eu^{3+} nanophosphors with >80% down conversion efficiency. *J. Mater. Chem. C* **2014**, doi:10.1039/C3TC31939C.

24. Dhanaraj, J.; Jagannathan, R.; Kutty, T.R.N.; Lu, C.-H. Photoluminescence characteristics of Y$_2$O$_3$: Eu^{3+} nanophosphors prepared using sol-gel thermolysis. *J. Phys. Chem. B* **2001**, *105*, 11098–11105.

25. Van Hao, B.; Huy, P.T.; Khiem, T.N.; Ngan, N.T.T.; Duong, P.H. Synthesis of Y$_2$O$_3$: Eu^{3+} micro-and nanophosphors by sol-gel process. *J. Phys. Conf. Series* **2009**, *187*, 12074.

26. Liu, F.; Yan, W.; Chuang, Y.-J.; Zhen, Z.; Xie, J.; Pan, Z. Photostimulated near-infrared persistent luminescence as a new optical read-out from Cr^{3+}-doped LiGa$_5$O$_8$. *Sci. Rep.* **2013**, doi:10.1038/srep01554.

27. Chuang, Y.-J.; Zhen, Z.; Zhang, F.; Liu, F.; Mishra, J.P.; Tang, W.; Chen, H.; Huang, X.; Wang, L.; Chen, X. Photostimulable Near-Infrared Persistent Luminescent Nanoprobes for Ultrasensitive and Longitudinal Deep-Tissue Bio-Imaging. *Theranostics* **2014**, *4*, 1112.

28. Ajithkumar, G.; Yoo, B.; Goral, D.E.; Hornsby, P.J.; Lin, A.-L.; Ladiwala, U.; Dravid, V.P.; Sardar, D.K. Multimodal bioimaging using a rare earth doped Gd$_2$O$_2$S:Yb/Er phosphor with upconversion luminescence and magnetic resonance properties. *J. Mater. Chem. B* **2013**, *1*, 1561–1572.

29. Li, L.; Zhang, R.; Yin, L.; Zheng, K.; Qin, W.; Selvin, P.R.; Lu, Y. Biomimetic Surface Engineering of Lanthanide-Doped Upconversion Nanoparticles as Versatile Bioprobes. *Angew. Chemie* **2012**, *124*, 6225–6229.

30. Sun, C.; Carpenter, C.; Pratx, G.; Xing, L. Facile synthesis of amine-functionalized Eu^{3+}-doped $La(OH)_3$ nanophosphors for bioimaging. *Nanoscale Res. Lett* **2011**, *6*, 24.

31. Cao, T.; Yang, T.; Gao, Y.; Yang, Y.; Hu, H.; Li, F. Water-soluble $NaYF_4$:Yb/Er upconversion nanophosphors: Synthesis, characteristics and application in bioimaging. *Inorg. Chem. Commun.* **2010**, *13*, 392–394.

32. Olesiak-Banska, J.; Nyk, M.; Kaczmarek, D.; Matczyszyn, K.; Pawlik, K.; Samoc, M. Synthesis and optical properties of water-soluble fluoride nanophosphors co-doped with Eu^{3+} and Tb^{3+}. *Opt. Mater. (Amst).* **2011**, *33*, 1419–1423.

33. Sun, Y.; Peng, J.; Feng, W.; Li, F. Upconversion nanophosphors $NaluF_4$:Yb, Tm for lymphatic imaging *in vivo* by real-time upconversion luminescence imaging under ambient light and high-resolution X-ray CT. *Theranostics* **2013**, *3*, 346.

34. Chen, J.-Y.; Huang, C.K.; Hung, W.B.; Sun, K.W.; Chen, T.M. Efficiency improvement of Si solar cells using metal-enhanced nanophosphor fluorescence. *Sol. Energy Mater. Sol. Cells* **2014**, *120*, 168–174.

35. Dhoble, S.J.; Shinde, K.N. Ce^{3+} and Eu^{3+} activtated $Na_2Sr_2Al_2PO_4F_9$ nanophosphor. *Adv. Mater. Lett.* **2011**, *2*, 349.

36. Yadav, R.S.; Pandey, S.K.; Pandey, A.C. Blue-Shift and Enhanced Photoluminescence in $BaMgAl_{10}O_{17}$:Eu^{2+} Nanophosphor under VUV Excitation for PDPs Application. *Mater. Sci. Appl.* **2010**, *1*, 25.

37. Niyaz Parvin, S.; Poornachandra Rao, N.V.; Subba Rao, B.; Murthy, K.V.R. Photoluminescence Studies on Sr_2CeO_4 Nanophosphor. *Wourld J. Chem.* **2011**, *6*, 114–117.

38. Minsung, K.; Makoto, K.; Hideki, K.; Masato, K. A Highly Luminous $LiCaPO_4$: Eu^{2+} Phosphor Synthesized by a Solution Method Employing a Water-Soluble Phosphate Ester. *Opt. Photonics J.* **2013**, doi:10.4236/opj.2013.36A003.

39. Zako, T.; Nagata, H.; Terada, N.; Sakono, M.; Soga, K.; Maeda, M. Improvement of dispersion stability and characterization of upconversion nanophosphors covalently modified with PEG as a fluorescence bioimaging probe. *J. Mater. Sci.* **2008**, *43*, 5325–5330.

40. Dong, K.; Ju, E.; Liu, J.; Han, X.; Ren, J.; Qu, X. Ultrasmall biomolecule-anchored hybrid GdVO 4 nanophosphors as a metabolizable multimodal bioimaging contrast agent. *Nanoscale* **2014**, *6*, 12042–12049.

41. Gao, K.; Jiang, X. Influence of particle size on transport of methotrexate across blood brain barrier by polysorbate 80-coated polybutylcyanoacrylate nanoparticles. *Int. J. Pharm.* **2006**, *310*, 213–219.

42. Chatterjee, K.; Sarkar, S.; Jagajjanani Rao, K.; Paria, S. Core/shell nanoparticles in biomedical applications. *Adv. Colloid Interface Sci.* **2014**, *209*, 8–39.

43. Yizhar, O.; Fenno, L.E.; Davidson, T.J.; Mogri, M.; Deisseroth, K. Optogenetics in neural systems. *Neuron* **2011**, *71*, 9–34.

44. Gupta, A.K.; Gupta, M. Synthesis and surface engineering of iron oxide nanoparticles for biomedical applications. *Biomaterials* **2005**, *26*, 3995–4021.

45. De la Fuente, J.M.; Berry, C.C.; Riehle, M.O.; Curtis, A.S.G. Nanoparticle targeting at cells. *Langmuir* **2006**, *22*, 3286–3293.

46. Zhou, Y.; Drummond, D.C.; Zou, H.; Hayes, M.E.; Adams, G.P.; Kirpotin, D.B.; Marks, J.D. Impact of single-chain Fv antibody fragment affinity on nanoparticle targeting of epidermal growth factor receptor-expressing tumor cells. *J. Mol. Biol.* **2007**, *371*, 934–947.

47. Dąbrowski, K.M.; Dul, D.T.; Korecki, P. X-ray imaging inside the focal spot of polycapillary optics using the coded aperture concept. *Opt. Express* **2013**, *21*, 2920–2927.

48. Romanov, A.Y. Optic parameters of a middle-focus Kumakhov lens for hard X-rays. *Tech. Phys. Lett.* **2005**, *31*, 200–201.

49. Cong, W.; Xi, Y.; Wang, G. X-Ray Fluorescence Computed Tomography With Polycapillary Focusing. *IEEE Access* **2014**, doi:10.1109/ACCESS.2014.2359831.

50. Di Fabrizio, E.; Romanato, F.; Gentili, M.; Cabrini, S.; Kaulich, B.; Susini, J.; Barrett, R. High-efficiency multilevel zone plates for keV X-rays. *Nature* **1999**, *401*, 895–898.

51. Nagel, G.; Szellas, T.; Huhn, W.; Kateriya, S.; Adeishvili, N.; Berthold, P.; Ollig, D.; Hegemann, P.; Bamberg, E. Channelrhodopsin-2, a directly light-gated cation-selective membrane channel. *Proc. Natl. Acad. Sci.* **2003**, *100*, 13940–13945.

52. Agrisera Antibodies Product Information. Available online: http://www.agrisera.com/cgi-bin/ibutik/SkapaFaktura.pl?SkrivPDF=J&funk=visa_artikel&artnr=AS121851&Friendly_Grupp=bacterial-insect-and-fungal-&Friendly=nphr-halorhodopsin-&artgrp=28&Sprak=en (accessed on 5 November 2014).

53. Uegaki, K.; Sugiyama, Y.; Mukohata, Y. Archaerhodopsin-2, from *Halobacterium* sp. aus-2 further reveals essential amino acid residues for light-driven proton pumps. *Arch. Biochem. Biophys.* **1991**, *286*, 107–110.

54. Erickson, H.P. Size and shape of protein molecules at the nanometer level determined by sedimentation, gel filtration, and electron microscopy. *Biol. Proced. Online* **2009**, *11*, 32–51.

55. Arenkiel, B.R.; Peca, J.; Davison, I.G.; Feliciano, C.; Deisseroth, K.; Augustine, G.J.; Ehlers, M.D.; Feng, G. *In vivo* light-induced activation of neural circuitry in transgenic mice expressing channelrhodopsin-2. *Neuron* **2007**, *54*, 205–218.

56. Mattis, J.; Tye, K.M.; Ferenczi, E.A.; Ramakrishnan, C.; O'Shea, D.J.; Prakash, R.; Gunaydin, L.A.; Hyun, M.; Fenno, L.E.; Gradinaru, V. Principles for applying optogenetic tools derived from direct comparative analysis of microbial opsins. *Nat. Methods* **2012**, *9*, 159–172.

57. Raimondo, J.V.; Kay, L.; Ellender, T.J.; Akerman, C.J. Optogenetic silencing strategies differ in their effects on inhibitory synaptic transmission. *Nat. Neurosci.* **2012**, *15*, 1102–1104.

58. Yue, G.Z.; Qiu, Q.; Gao, B.; Cheng, Y.; Zhang, J.; Shimoda, H.; Chang, S.; Lu, J.P.; Zhou, O. Generation of continuous and pulsed diagnostic imaging x-ray radiation using a carbon-nanotube-based field-emission cathode. *Appl. Phys. Lett.* **2002**, *81*, 355.

59. Radiation Dose in X-Ray and CT Exams. Available online: http://www.radiologyinfo.org/en/safety/?pg=sfty_xray (accessed on 27 October 2014).

60. Energy and Work Unit Conversion. Available online: http://www.unit-conversion.info/energy.html (accessed on 10 November 2014).

61. Hegemann, P.; Möglich, A. Channelrhodopsin engineering and exploration of new optogenetic tools. *Nat. Methods* **2011**, *8*, 39–42.

62. Frenzel, J.; Schultes, H. Luminescence in water carrying supersonic waves. *Z. Phys. C* **1934**, *27*, 421–424.

63. Hilgenfeldt, S.; Grossmann, S.; Lohse, D. A simple explanation of light emission in sonoluminescence. *Nature* **1999**, *398*, 402–405.

64. Zhou, J.; Xing, D.; Chen, Q. Enhancement of Fluoresceinyl Cypridina Luciferin Analog Chemiluminescence by Human Serum Albumin for Singlet Oxygen Detection. *Photochem. Photobiol.* **2006**, *82*, 1058.

65. Christensen, D.A. *Ultrasonic bioinstrumentation*; JW Sons: New York, NY, USA, 1988.

66. Shen, C.; Xu, J.; Fang, N.X.; Jing, Y. Anisotropic Complementary Acoustic Metamaterial for Canceling out Aberrating Layers. *Phys. Rev. X* **2014**, *4*, 41033.

67. Jia, Z.; Valiunas, V.; Lu, Z.; Bien, H.; Liu, H.; Wang, H.-Z.; Rosati, B.; Brink, P.R.; Cohen, I.S.; Entcheva, E. Stimulating Cardiac Muscle by Light Cardiac Optogenetics by Cell Delivery. *Circ. Arrhythmia Electrophysiol.* **2011**, *4*, 753–760.

68. Berndt, A.; Lee, S. Y.; Ramakrishnan, C.; Deisseroth, K. Structure-Guided Transformation of Channelrhodopsin into a Light-Activated Chloride Channel. *Science (80-.).* **2014**, *344*, 420–424.

69. Zhang, J.; Yang, G.; Cheng, Y.; Gao, B.; Qiu, Q.; Lee, Y.Z.; Lu, J.P.; Zhou, O. Stationary scanning x-ray source based on carbon nanotube field emitters. *Appl. Phys. Lett.* **2005**, *86*, 184104.